J Solid State Electrochem (2010) 14:585–591
DOI 10.1007/s10008-009-0815-4

ORIGINAL PAPER

Electrochemical and structural characterization of lithium titanate electrodes

Ping Liu · Elena Sherman · Mark Verbrugge

Received: 7 January 2009 / Accepted: 20 February 2009 / Published online: 7 March 2009

Abstract Lithium titanate (LTO) materials of different particle size, surface area, and morphology were characterized by constant current cycling and cyclic voltammetry. By examining the particles and electrodes with scanning electron microscopy, we show that particle morphology, in addition to particle size, has important implications for high-rate performance. Large agglomerates, even when porous and made of small crystallites, cannot effectively form homogenous electrodes with the polymer binder and carbon conducting diluents; hence, low power performance results. Another nanostructured LTO of very high surface area was found to have poor electrochemical performance most likely due to its high concentration of structural defects. We recommend further development in nanoparticles of LTO of optimal crystallinity as well as improved electrode homogeneity through the use of more compatible binders and conducting diluents and better electrode processing techniques. Simultaneous realization of these imperatives should facilitate the development of LTO-based high-power batteries for automotive applications.

Keywords Lithium ion battery · Anode material · Lithium titanate · Scanning electron microscopy · Nanoparticle

P. Liu (✉) · E. Sherman
HRL Laboratories LLC,
Malibu, CA 90265, USA
e-mail: pliu@hrl.com

M. Verbrugge
General Motors Corporation,
Warren, MI 48090, USA

Introduction

Lithium ion batteries with lithium titanate (LTO) as the anode have been suggested recently for automotive traction applications [1–6]. These batteries promise high power, enhanced abuse tolerance, and long cycle life. LTO experiences very little volume change during battery cycling, which leads to its outstanding cycling stability. The working potential of LTO is ~1.5 V versus lithium metal, which makes it possible to use very small particles, including nanoparticles, to offer very high power capabilities without raising abuse-tolerance concerns associated with solvent reactions over the electrode surface.

There are extensive reports on methods to synthesize LTO with different size and morphology [7–19]. In addition to traditional solid-state methods [13], several of these reports use variations of the sol–gel method [7, 11, 20]. Approaches to synthesizing nanoparticles of LTO are also diverse, ranging from solid-state [11] to sonochemical [21] methods. The use of nanoparticles promises high-power capabilities due to reduced solid state diffusion length for lithium ions. An alternative approach to achieve the same goal is to use highly porous materials with very thin walls [12, 14].

In order to develop material structure–property relationship, most of these materials were evaluated in liquid electrolyte cells after being fabricated into electrodes by adding a conducting diluent and a polymer binder. While the particle size and morphology were often characterized by scanning electron microscopy, the microstructure of the fabricated electrode was not as widely reported. Lithium titanate is an electronic insulator, which makes it critical to establish intimate contact with the conducting diluents. The resulting electronic conductivity, in combination with the

reduced solid state diffusion length, should lead to good high-power performance.

The purpose of the current study is to understand the effect of particle size, morphology, and crystallinity on the electrochemical performance of LTO materials that will serve as the basis for analysis of lithium ion batteries with LTO as the anode. In particular, we are interested in learning how the particle properties affect the microstructure of electrodes, which in turn impacts the electrochemical performance. Our study also illustrates the challenges in realizing the full benefits of nanomaterials in lithium ion batteries.

Experimental

Four LTO samples were evaluated in this work. Electrodes were cast using the doctor-blade technique from a slurry of LTO, carbon black (Super P®, Timcal), polyvinylidene diflouride (PVDF) binder dissolved in acetone, and propylene carbonate. Circular disks were extracted from of the tape and dried at 100 °C for 12 h under vacuum. The final electrode composition was 70% LTO, 10% carbon black, and 20% PVDF. The electrodes were tested in Swagelok cells with lithium as both the counter and reference electrodes. The electrolyte solution was 1 M $LiPF_6$ in EC/DMC/EMC/PC (4:3:2:1 *v*/*v*). Constant current cycling was performed on an Arbin battery testing station. The cycling voltage range was between 1 and 3 V versus Li/Li^+. Cyclic voltammograms were obtained on a 1255 Solartron Electrochemical Interface. Scanning electron microscopic images were acquired on a Hitachi S4800 system.

Results and discussion

Table 1 summarizes the large variation in medium particle size (d_{50}) and BET surface area for the four materials investigated. LTO4 has a noticeably high surface area along with a small d_{50} value of 200 nm. LTO1–3 are quite similar with LTO3 having the smallest surface area. These four materials thus make it possible to perform comparisons with regard to particle size and surface area. All materials were examined by X-ray diffraction, which confirmed their spinel structure (Fig. 1). LTO4 has extremely broad peak patterns indicative of nanocrystalline domains in the material.

Table 1 Summary of LTO materials in this study

LTO	d_{50} (μm)	BET (m^2/g)	C/4 capacity (mA h/g)
1	21.0	2.9	174.0
2	9.4	2.9	155.1
3	18.7	1.0	166.2
4	0.2	84.8	150.5

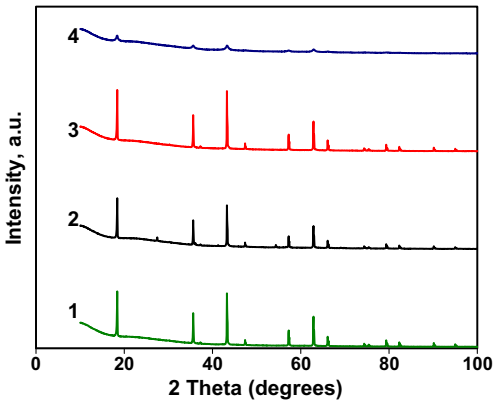

Fig. 1 X-ray diffraction patterns of four lithium titanate materials examined in this paper. All of the materials have patterns consistent with a spinel structure. LTO4's weak and broad patterns are indicative of its nanocrystalline structure

Constant current cycling is performed at 0.25, 0.5, 1, 2, and 4 mA/cm^2 for a total of 100 cycles. Figure 2 shows the discharge curves for all materials at different rates. At a current density of 0.25 mA/cm^2 or a rate of ~C/4, all materials deliver similar capacities of 150–170 mA h/g as listed in Table 1. Their high-rate performance varies greatly, however. We notice a couple of interesting contrasts. First, LTO1 and 2 seem to only differ in medium particle size with identical surface area. However, LTO2 shows substantially better high-rate performance than LTO1. At 4 mA/cm^2, LTO2 delivers a capacity of 90 versus 70 mA h/g for LTO1. Second, LTO4 has very small particle sizes with large surface area. However, its electrochemical performance is rather poor. Its less developed voltage plateau on discharge is consistent with the material being nanocrystalline, but its high-rate performance is worse than any of the other materials despite the small particle size and associated short diffusion length within the particle. The capacity retention of the four materials is shown in Fig. 3. Good cycling stability is observed for LTO2 and 3, while both 1 and 4 experienced much faster capacity fade. In particular, the capacity loss appears to increase significantly at the highest discharge rate for LTO1.

We also characterized the electrode reactions with cyclic voltammetry at 100 mV/s as shown in Fig. 4. The most noticeable feature is the poor kinetics of LTO4. When the anodic scan returns to 3 V, the residual current indicates incomplete removal of lithium from the electrode. In contrast, none of the other materials suffer from this hysterisis. In addition, the peak current of LTO1 is also noticeably lower than LTO2 and 3, indicative of poor performance at this high rate.

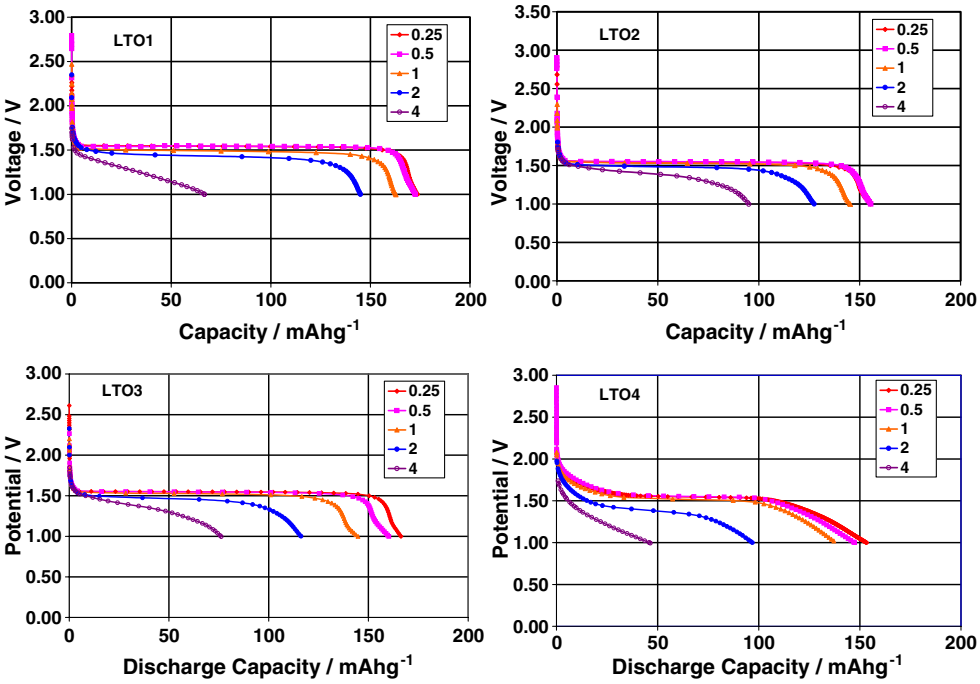

Fig. 2 Charge–discharge curves at five different rates for lithium titanate electrodes. The legends are current densities with the units being mA cm^{-2}

Our electrochemical data so far seem to contradict a common conception that particle size is largely responsible for electrochemical rate performance since it directly determines the length of solid state diffusion. We subsequently examined the morphology of the four materials to seek an explanation. Figures 5 and 6 show low- and high-magnification scanning electron microscopy images for the four materials. Despite the identical BET surface area with d_{50} values differing by a factor of two, LTO1 and 2 have very different morphologies. LTO1 is composed of spherical particles of different sizes with the largest being ~30 μm. In contrast, LTO2 appears to have much smaller particle size. This apparent contradiction can be better understood from the high-resolution images in Fig. 6. The spherical particles of LTO are in fact made of small crystallites, of dimension less than 1 μm. Many of the particles also have octahedron shapes, typical for single crystals of a spinel material. These small crystallites form porous agglomerates, which still possess similar to even higher surface area than LTO2 or 3. Indeed, the high-resolution images of LTO2 and 3 show that they have crystallites clearly larger than LTO1. Due to their

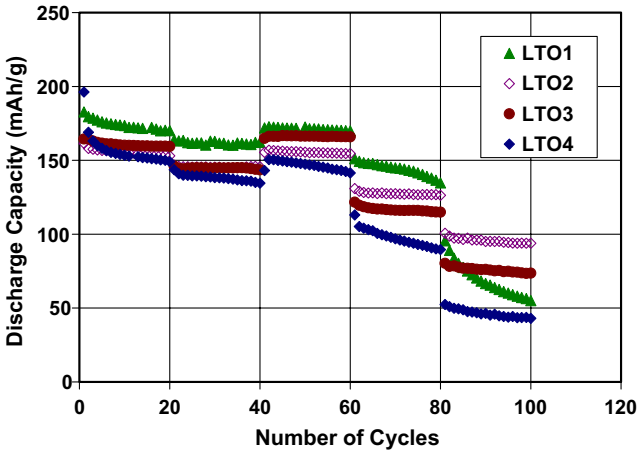

Fig. 3 Capacity retention for LTO1–4 during constant current cycling. The current densities are in the order of 0.5, 1, 0.25, 2, and 4 mA cm^{-2} for every incremental 20 cycles

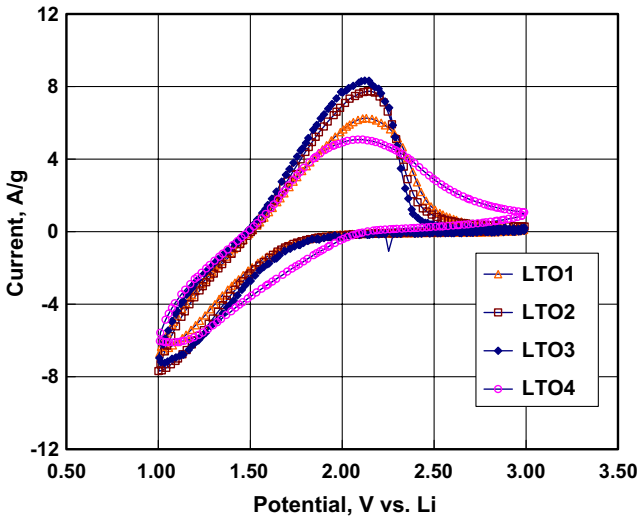

Fig. 4 Cyclic voltammograms of lithium titanate electrodes at scan rates of 100 mV/s

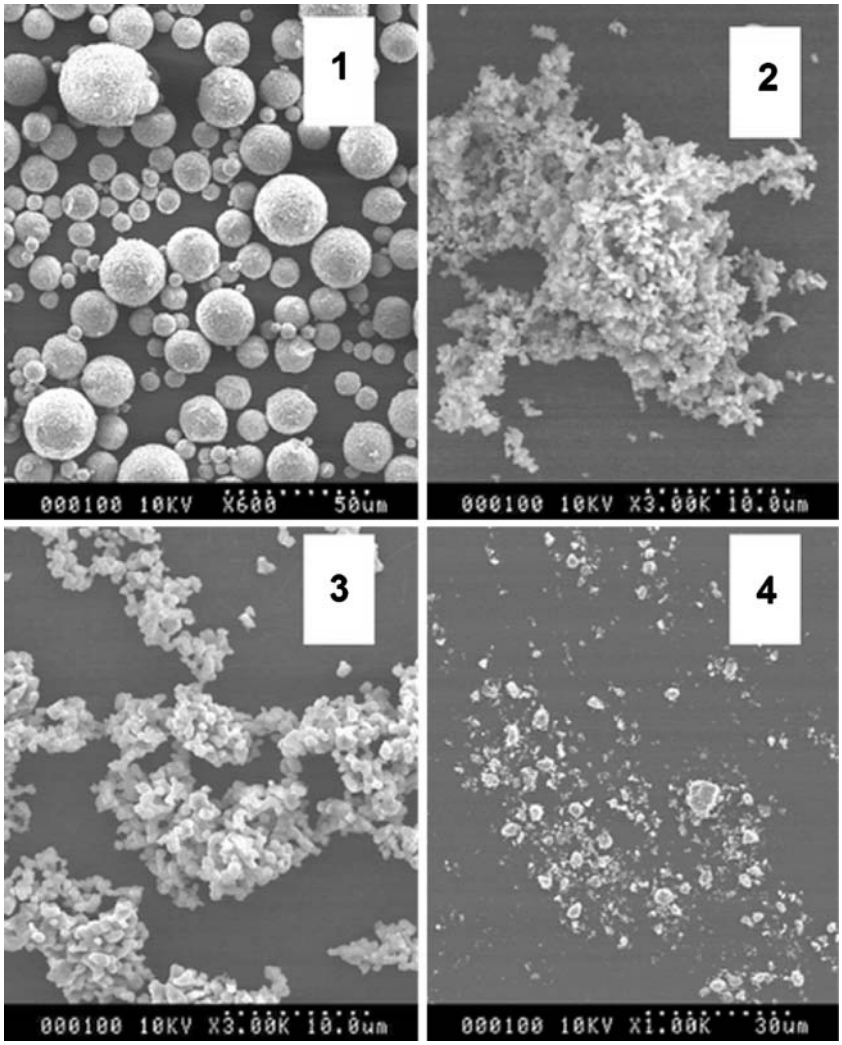

Fig. 5 Scanning electron microscopy images of lithium titanate materials at low magnification. LTO1 is composed of spherical particles of different sizes

similar morphology, the larger crystallite size in LTO3 than LTO2 is consistent with its lower surface area and larger d_{50}. Finally, LTO4 does not show the crystallite features observed in all other materials despite the broad XRD patterns showing the spinel structure.

We further examined the morphology of the LTO/carbon/PVDF composite electrode to see how it correlates with particle morphology. Figures 7 and 8 show low- and high-resolution images, respectively. During electrode processing of LTO1, the spherical particles were preserved in the electrode as shown in Fig. 7. While carbon apparently coats most of the large particles, the electrode is highly inhomogeneous. LTO2–4 appear to have substantially better homogeneity. The effectiveness of carbon coating of LTO is better illustrated in the high-resolution images of Fig. 8. In LTO1, the carbon/polymer additive is only in contact with a portion of the LTO particle surface and does not appear to have penetrated into the interior of the larger particle. Better mixing is observed in LTO2 to 4 with the homogeneity in LTO4 being the best. In general, however, carbon/PVDF appears to have failed in coating the LTO crystallites effectively, indicative of a large surface energy mismatch.

We can now better explain the difference in high-rate electrochemical performance between these materials. While LTO1 has similar surface area as LTO2, its unique porous spherical morphology was preserved in the electrode. When combined with ineffective coating of the oxide surface by carbon/PVDF and a lack of penetration of the interior of the spherical particles, the LTO in the electrode lacks sufficient electronic conduction to deliver high power. LTO2 and 3 have very similar particle and electrode morphology. However, the crystallite size in LTO3 is larger, which could explain its inferior high-rate performance as compared to LTO2. Finally, LTO4 has very small particles with apparently good compatibility with the carbon/PVDF.

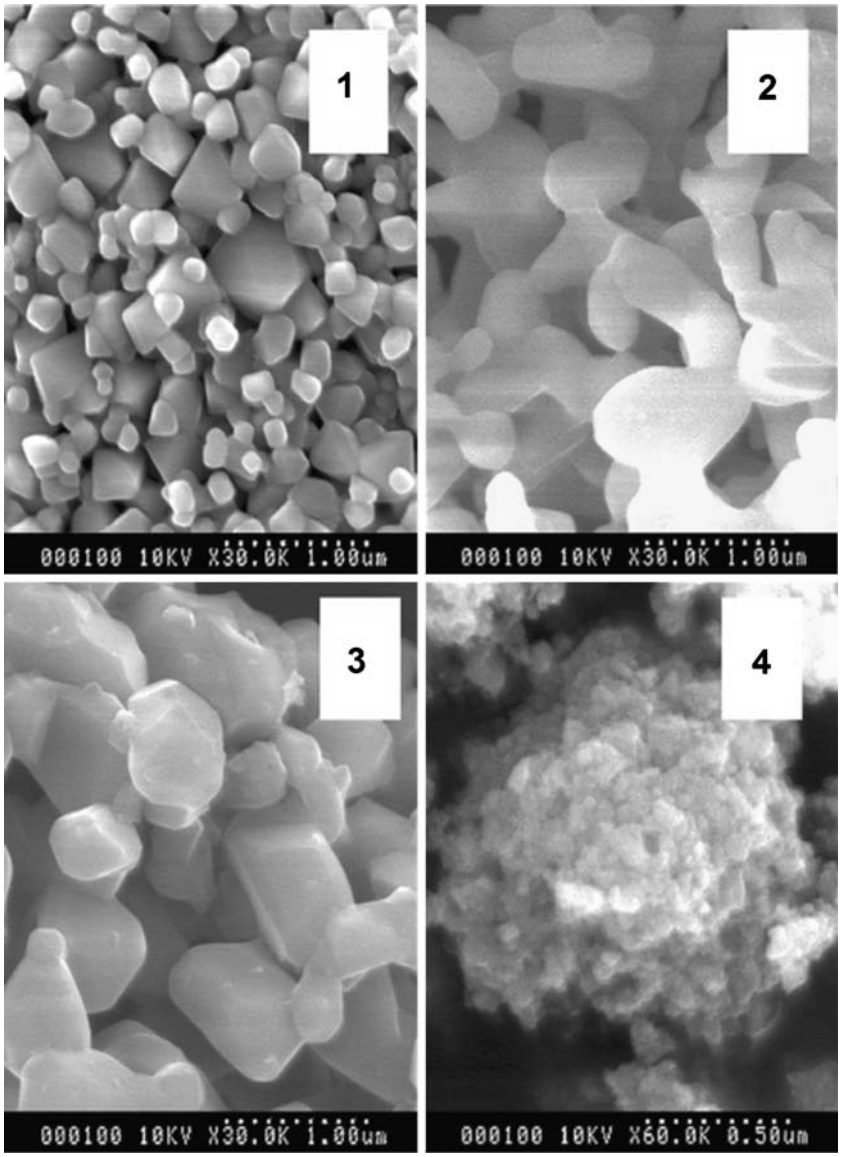

Fig. 6 Scanning electron microscopy images of lithium titanate materials at high magnification. LTO1–3 are all made of small crystallites despite their difference in morphology shown in Fig. 4. The nanocrystallines in LTO4 are difficult to see

Its poor high-rate performance is most likely a result of large amounts of structural or surface defects, which would help to explain the great hysteresis during cyclic voltammetry as shown in Fig. 5. During the synthesis of nanoparticles, they are often prevented from extended exposure to high temperature to avoid sintering. However, this procedure can also lead to insufficient crystallization and large amount of defects.

Conclusions

Our work shows that particle size, morphology, and crystallinity are all important factors affecting rate and cycling stability of lithium titanate materials. The spherical particles, despite being porous and made of small crystallites, do not provide the best high-rate performance. When particle agglomarization behavior is similar, smaller crystallites provide better high-rate performance. The sensitivity to particle morphology is largely due to the poor surface compatibility between the oxide and the carbon/polymer composite used in this study. The nanosized LTO4 shows inferior electrochemical performance to other materials, perhaps due to large amount of structural defects. We recommend further development in nanoparticles of LTO of optimal crystallinity as well as improved electrode homogeneity through the use of more compatible binders or conducting diluants and better processing techniques. Simultaneous realization of these imperatives will pave the way for LTO-based high-power batteries for automotive applications.

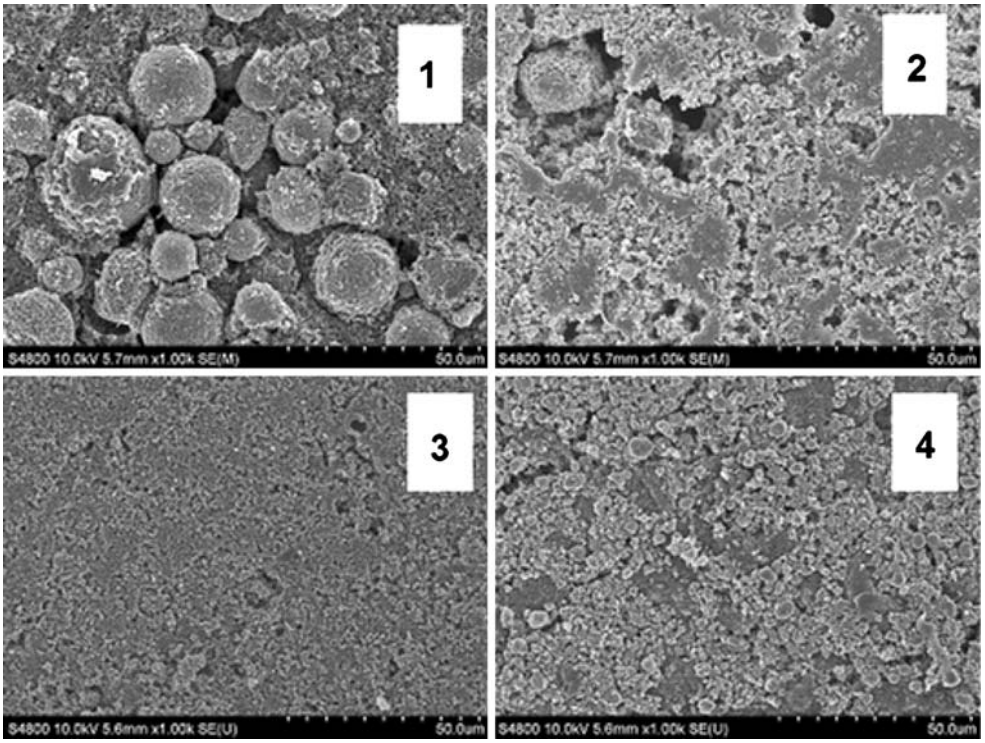

Fig. 7 Scanning electron microscopy images of electrodes at low magnification. The spherical particle morphology was preserved during electrode processing

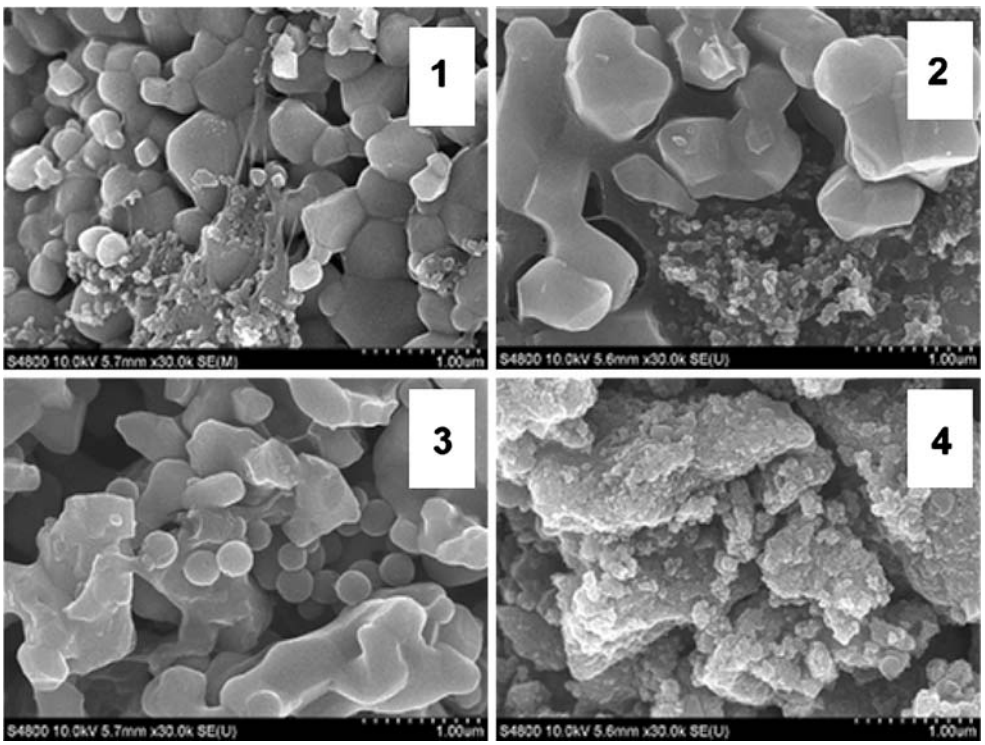

Fig. 8 Scanning electron microscopy images of lithium titanate electrodes at high magnification. Poor dispersion of PVDF and carbon on LTO surface is seen on LTO1–3

References

1. Gotcher A (2005) Adv Mater Process 163:32
2. Verbrugge MW, Liu P (2007) J Power Sources 174:2. doi:10.1016/j.jpowsour.2007.03.019
3. Du Pasquier A, Plitz I, Menocal S, Amatucci G (2003) J Power Sources 115:171. doi:10.1016/s0378-7753(02) 00718-8
4. Plitz I, DuPasquier A, Badway F et al (2006) Appl Phys A Mater Sci Process 82:615. doi:10.1007/s00339-005-3420-0
5. Du Pasquier A, Plitz I, Gural J, Badway F, Amatucci GG (2004) J Power Sources 136:160. doi:10.1016/j.jpowsour.2004.05.023
6. Stewart S, Albertus P, Srinivasan V et al (2008) J Electrochem Soc 155:A253. doi:10.1149/1.2830552
7. Bach S, Pereira-Ramos JP, Baffier N (1998) J Mater Chem 8:251. doi:10.1039/a706388a
8. Gao J, Jiang CY, Ying JR, Wan CR (2006) J Power Sources 155:364
9. Gao J, Ying JR, Jiang CY, Wan CR (2007) J Power Sources 166:255. doi:10.1016/j.jpowsour.2007.01.014
10. Guerfi A, Sevigny S, Lagace M, Hovington P, Kinoshita K, Zaghib K (2003) J Power Sources 119:88. doi:10.1016/S0378-7753(03) 00131-9
11. Hao YJ, Lai QY, Lu JZ, Wang HL, Chen YD, Ji XY (2006) J Power Sources 158:1358. doi:10.1016/j.jpowsour.2005.09.063
12. Jiang CH, Zhou Y, Honma I, Kudo T, Zhou HS (2007) J Power Sources 166:514. doi:10.1016/j.jpowsour.2007.01.065
13. Ohzuku T, Ueda A, Yamamoto N (1995) J Electrochem Soc 142:1431. doi:10.1149/1.2048592
14. Sorensen EM, Barry SJ, Jung HK, Rondinelli JR, Vaughey JT, Poeppelmeier KR (2006) Chem Mater 18:482. doi:10.1021/cm052203y
15. Wu L, Kan SR, Lu SG, Zhang XJ, Jin WH (2007) Trans Nonferrous Met Soc China 17:S117
16. Zaghib K, Simoneau M, Armand M, Gauthier M (1999) J Power Sources 82:300. doi:10.1016/S0378-7753(99) 00209-8
17. Guerfi A, Charest P, Kinoshita K, Perrier M, Zaghib K (2004) J Power Sources 126:163. doi:10.1016/j.jpowsour.2003.08.045 doi:10.1016/j.jpowsour.2003.08.045
18. Julien CM, Zaghib K (2004) Electrochim Acta 50:411. doi:10.1016/j.electacta.2004.03.052
19. Matsui E, Abe Y, Senna M, Guerfi A, Zaghib K (2008) J Am Ceram Soc 91:1522. doi:10.1111/j.1551-2916.2008.02269.x
20. Bach S, Pereira-Ramos JP, Baffier N (1999) J Power Sources 82:273. doi:10.1016/S0378-7753(98) 00216-X
21. Lee SS, Byun KT, Park JP, Kim SK, Kwak HY, Shim IW (2007) Dalton Trans 4182–4184. doi:10.1039/b707164g